



Full Text View

[Volume 29, Issue 8 \(August 1999\)](#)

Journal of Physical Oceanography

Article: pp. 1801–1811 | [Abstract](#) | [PDF \(171K\)](#)

Wind Speed Scaling in Fully Developed Seas

Donald T. Resio

U.S. Army Corps of Engineers Waterways Experiment Station, Vicksburg, Mississippi

Val R. Swail

Environment Canada, Downsview, Ontario, Canada

Robert E. Jensen

U.S. Army Corps of Engineers Waterways Experiment Station, Vicksburg, Mississippi

Vincent J. Cardone

Oceanweather, Inc., Cos Cob, Connecticut

(Manuscript received January 6, 1997, in final form August 17, 1998)

DOI: 10.1175/1520-0485(1999)029<1801:WSSIFD>2.0.CO;2

ABSTRACT

Recent tests of all generations of numerical wave models indicate that extreme wave heights are significantly underpredicted by these models. This behavior is consistent with the finding by Ewing and Laing that fully developed wave spectra do not have the universal self-similar form postulated by Pierson and Moskowitz. This paper postulates that it is inappropriate to scale fully developed seas by winds taken from a fixed level above the mean sea surface. Instead, winds should be taken from a dynamically scaled height that is linearly related to the wavelength of the spectral peak. This alternative scaling is consistent with friction-velocity scaling and yields predicted wave heights and periods that are in better agreement with the data collected by Ewing and Laing and appear to explain some of the discrepancies in results from previous studies with numerical wave models in large storms.

1. Introduction

In a recent paper, [Cardone et al. \(1996\)](#) show that modern wave prediction

Table of Contents:

- [Introduction](#)
- [Theoretical perspective](#)
- [Results and discussion](#)
- [Conclusions](#)
- [REFERENCES](#)
- [FIGURES](#)

Options:

- [Create Reference](#)
- [Email this Article](#)
- [Add to MyArchive](#)
- [Search AMS Glossary](#)

Search CrossRef for:

- [Articles Citing This Article](#)

Search Google Scholar for:

- [Donald T. Resio](#)

models (first generation, second generation, and third generation) all appear to predict significant wave heights up to about 12 m in the open ocean with little or no bias. For wave heights higher than this, all three generations of wave models significantly underpredicted extreme sea states in the two major storms studied in that paper. Although it is possible that the synoptic-scale winds used in the hindcast studies were biased low, considerable effort was expended to minimize any such tendency. An interesting possibility in light of this finding is that all three generations of wave models may contain an inherent tendency to underpredict waves in sea states above 12 m. Since today's numerical wave prediction models are utilized in the estimation of design conditions for offshore and coastal structures and in scheduling operations on a worldwide basis, this finding is not only of interest to researchers but is also potentially of critical interest to a wide range of applications around the globe.

- [Val R. Swail](#)
- [Robert E. Jensen](#)
- [Vincent J. Cardone](#)

In the mid-1960s, a series of papers established a strong foundation for the form of wave spectra for fully developed seas ([Pierson and Moskowitz 1964](#)). Although considerable effort has been expended on modeling wave conditions that incorporate various forms of fully developed criteria, little additional observational evidence was examined since those early studies until a study by Ewing and Laing in 1987. This effort examined a set of carefully screened spectra taken from a location off the southwest coast of the British Isles. Ewing and Laing found that for wind speeds below about 16 m s^{-1} , measured spectral energies fell consistently under the generally accepted Pierson–Moskowitz values. For wind speeds above about 16 m s^{-1} , spectral energies were similar to the Pierson–Moskowitz values.

Today's wave models use wind speeds measured at a fixed height (typically 10 m) above the mean water level, along with derived wind stresses, to characterize wind input into the wave field. As discussed by [Komen et al. \(1984\)](#), two alternative scaling laws have been advocated for wind inputs: scaling with friction velocity and scaling with wind speeds at a fraction of a wavelength above the sea surface. It will be shown here, specifically for the case of fully developed wave conditions, that respecification of input winds at a dynamically scaled height above the sea surface appears to be more consistent with the physics of wave generation and seems to produce results that might explain some of the apparent discrepancies in the Ewing and Laing data. Also, the ratio of fully developed wave heights based on dynamic-height scaling of the wind to wave heights based on winds from a constant elevation are consistent with observed biases from the [Cardone et al. \(1996\)](#) and [Khandekar et al. \(1994\)](#) hindcast comparisons. Furthermore, it will be shown that this type of scaling is consistent with a friction–velocity scaling for fully developed seas.

2. Theoretical perspective

Even though the existence of a steady-state, fully developed wind sea has never been definitively established, scientists and engineers have made use of this concept in virtually all wave prediction models developed in the twentieth century. [Sverdrup and Munk \(1947\)](#), [Bretschneider \(1952\)](#), and [Pierson et al. \(1955\)](#) provide three good examples of early parametric wave models that incorporate an explicit upper limit to wave development as a function of wind speed. Subsequent spectral wave models have all retained some form of this constraint in their formulations. For example, first- and second-generation wave models ([Bunting 1970](#); [Barnett 1968](#); [Resio 1981](#)) incorporate this limit explicitly via constraints on the minimum frequency that can receive energy directly from the wind; and third-generation wave models ([WAMDI 1988](#)) incorporate this limit indirectly through calibrations to fully developed scenarios ([Komen et al. 1984](#)). An important point to note, however, is that such models are not constrained to follow any particular growth law or fully developed limit based on similarity theory, since they are formulated in terms of physics-based sources and sinks rather than similarity principles.

The justification for the existence of fully developed sea states in wave generation has generally been based on the following considerations. First, it has been observed that, during low wind conditions, waves do not continue to grow, but rather appear to approach some asymptotic upper limit. Second, the concept of similarity relationships among wind and wave parameters, as established by [Kitaigorodskii \(1962\)](#), and extended by [Pierson and Moskowitz \(1964\)](#), suggests that certain scaling relationships should exist for this case. And third, essentially all theoretical concepts of wind inputs into waves have forms such that as the phase speed of waves approaches the wind speed, direct transfer of momentum from the wind to the wave field ceases (e.g., [Miles 1957](#); [Chalikov 1976](#); [Janssen 1991](#); [Jenkins 1993](#)).

An early hypothesis for fully developed sea conditions came from [Sverdrup and Munk \(1947\)](#), who suggested that a fixed relationship exists between wave heights and the wind speeds,

$$H_{s\text{-fd}} = \lambda \frac{u^2}{g}, \quad (1)$$

where λ is a dimensionless constant, u is wind speed, g is gravity, and $H_{s\text{-fd}}$ is the fully developed significant wave height, related to energy in the fully developed waves $E_{s\text{-fd}}$ by

$$H_{s\text{-fd}} \approx 4(E_{s\text{-fd}})^{1/2}.(2)$$

[Pierson and Moskowitz \(1964\)](#) provided some early empirical support for both the existence of a fully developed limit to wave growth and a corresponding spectral shape, which has since been termed the Pierson–Moskowitz spectrum. In their formulation, the peak frequency of a growing sea would asymptotically approach a low-frequency limit given by

$$f_{\text{PM}} = \frac{\nu g}{u}, \quad (3)$$

where f_{PM} is the limiting frequency for a Pierson–Moskowitz spectrum and ν is an empirical constant. In terms of a wind speed taken at a constant elevation above the water surface of 10 m, the value of ν is typically taken to be approximately 0.13 ([Pierson 1977](#)).

As pointed out previously, in first- and second-generation wave models, a cutoff frequency for wave growth is explicitly included within the wave generation algorithms used. In an attempt to overcome such direct constraints in wave models, there has been an international effort to produce a wave model based on the principle of detailed balance ([WAMDI 1988](#)). In these third-generation models side constraints on wave growth are relaxed and in some cases removed completely; and wave growth is modeled via the radiative transfer equation

$$\frac{\partial E(f, \theta)}{\partial t} = \mathbf{c}_g \cdot \nabla E(f, \theta) + \sum_{k=1}^3 S_k(f, \theta), \quad (4)$$

where $E(f, \theta)$ is the energy density in the spectrum at frequency f and propagation direction θ , \mathbf{c}_g is the group velocity, and $S_k(f, \theta)$ is the rate of energy gain or loss due to the k th source term at frequency f and direction θ . Conventionally, three source terms are considered to dominate wave growth in deep water ([WAMDI 1988](#)): wind input (S_{in}), nonlinear wave–wave interactions (S_{nl}), and wave breaking (S_{ds}).

Detailed knowledge of the physics governing the fully developed limit of wave growth is incomplete. For example, the wind input term is taken from a series of experiments ([Snyder and Cox 1966](#); [Snyder et al. 1981](#)) that concentrated on the specification of the wind source term during periods of active wave growth, rather than on the fully developed limit. Thus, we must make some ad hoc assumptions regarding the asymptotic behavior of S_{in} for fully developed seas when we incorporate S_{in} into a wave model. Furthermore, even assuming the wind source terms were known precisely and that the nonlinear interaction source term is governed exactly by the four-wave interaction form by [Hasselmann \(1962\)](#), we are still left with one term, wave breaking, which has not been well developed either theoretically or empirically. Consequently, detailed-balance models are not applied independently to establish criteria for fully developed seas, but are instead calibrated to match empirical evidence ([Komen et al. 1984](#)).

[Ewing and Laing \(1987\)](#) assembled a set of open-ocean spectra carefully selected to represent fully developed conditions. In the self-similar spectral form postulated by the [Pierson and Moskowitz \(1964\)](#), the nondimensional energy density $E(f)g^3/u^5$ in a spectrum should be a universal function of nondimensional frequency uf/g , that is,

$$\frac{E(f)g^3}{u^5} = \xi\left(\frac{uf}{g}\right).$$

[Figure 1](#) shows a comparison of this theoretical form to observations taken from [Ewing and Laing \(1987\)](#). As pointed out in their paper, for lower wind speeds the theoretical Pierson–Moskowitz form overpredicts the observed spectral densities, and for higher wind speeds it yields comparable values to those observed.

From [Eq. \(3\)](#), the value of ν ($=uf_{\text{PM}}/u$) is expected to be a universal constant, in the neighborhood of 0.13. If we plot ν against u_{10} from the Ewing and Laing data, we see that ν does not seem to be a constant as required for a self-similar wave-generation process ([Fig. 2](#)), but rather appears to decrease as wind speed increases. The only marked departure from this pattern occurs in Ewing and Laing’s lowest wind speed category ($u_{10} < 10 \text{ m s}^{-1}$).

In Fig. 2, the open circles denote cases with wind speeds greater than 10 m s^{-1} . The solid circles denote cases for lower wind speeds. A dashed line is used in this figure to emphasize the separation point. Cases with wind speeds less than 10 m s^{-1} do not follow as clear of a trend with wind speed as do cases with wind speeds higher than 10 m s^{-1} . Since most practical concerns for fully developed seas relate to conditions with wind speeds higher than 10 m s^{-1} , the regression line in this figure represents a best fit to only the stratified dataset (wind speeds greater than 10 m s^{-1}). This is consistent with studies by Pierson (1964) and Pierson and Moskowitz (1964), who also excluded situations with wind speeds under 20 knots (approximately 10 m s^{-1}). Only five data points are removed from the Ewing and Laing dataset by this exclusion; however, regression slopes are affected substantially, since cases with wind speeds under 10 m s^{-1} appear to deviate significantly from the $v-u_{10}$ relationship exhibited at higher wind speeds. The correlation coefficient between v and u_{10} is 0.49 for the stratified dataset, significant at the 0.005 level. The correlation coefficient between v and u_{10} for the entire dataset is 0.275, significant at the 0.05 level. The slope of the regression line for the stratified dataset is -0.0028 , while with the entire dataset the slope is -0.0014 , which is a reduction of a factor of 2 from the stratified dataset. All regression lines in subsequent plots will also be based only on cases with wind speed greater than 10 m s^{-1} , in order to maximize the fit to that part of the distribution. However, all of the data will be shown on each plot for completeness.

From the preceding analysis, we see that v , based on winds at a constant height of 10 m, appears not to be a universal constant. This is actually not that surprising since, in most applications of similarity theory in meteorology, the wind speed used for scaling purposes is taken as the speed at the top of the boundary layer, rather than at an arbitrary level within the boundary layer. Thus, from meteorological scaling considerations, as originally suggested by Kitaigorodskii (1962), it would seem that the wind speed above the effects of the wave field at the surface should be used for scaling wind-wave relationships. However, even in a neutral, barotropic atmosphere, the ratio of the wind speed at a fixed reference level to the wind speed at the top of the boundary layer is not a constant, but rather depends on the surface Rossby number, which is a function of the Coriolis parameter. Since there is little or no evidence supporting any relationship between wave generation and Coriolis effects, it is not clear that the wind speed at the top of the boundary layer is indeed the best choice for scaling fully developed wave spectra, particularly since most wave-generation processes occur very close to the ocean surface. Consequently, we will tentatively assume that the upper portion of the winds in the planetary boundary layer do not contribute directly to wave growth and will seek an appropriate scaling relationship based on some length scale within the boundary layer.

Miles (1957) theorized that the dominant stage of wave growth was controlled by the transfer of momentum from a “matched layer” within the wind profile into a given component of the wave field. This “matched layer” was located at a level above the surface such that the mean wind speed at that level was equal to the phase speed of the wave component into which the momentum was being transferred. In this context, a consistent scaling height for the wind speed might be taken as some fixed ratio of the wavelength above the surface. Since the wavelength of the spectral peak in a fully developed spectrum is strongly dependent on wind speed, the reference height for fully developed winds would also be expected to vary with wind speed.

A variation on the scaling approach has been previously suggested by Donelan and Pierson (1987), who hypothesized that the wind speed at a reference level of $L_p/2$, where L_p is the wavelength of the spectral peak frequency, might provide a more general scaling parameter for wind inputs than the wind speed at a fixed level. However, in this paper we make a clear distinction between wind parameters used during active wave growth and wind parameters used for characterizing fully developed seas. During active wave growth, it is expected that friction velocity will be the primary parameter affecting energy transfers from the atmosphere into the sea surface. Since friction velocity can be estimated from wind speeds measured at any height above the surface (given suitable estimates of surface roughness and atmospheric stability), the choice of wind measurement level during periods of active wave growth would seem to be somewhat arbitrary.

In a neutrally stable atmosphere, the solution for the wind speed at a reference level of λL_p above the sea surface, where λ is an empirical constant, can be accomplished via the combination of standard boundary layer equations. From the equation for the near-surface wind speed in a neutral boundary layer, we have

$$u = \frac{u^*}{k} \ln(z/z_0), \quad (5)$$

where k is Von Kármán’s constant (taken here as 0.4), z is the height at which the wind is taken, and z_0 is the characteristic roughness height of the surface. Hence, the ratio of wind speeds at two different levels is given by

$$\frac{u_{10}}{u_r} = \frac{10}{\ln\left(\frac{z_r}{z_0}\right)}, \quad (6)$$

where the subscripts “10” and “r” refer to the two different levels above the surface, the “10-meter” and the wave-length-scaled “reference” level ($z_r = \lambda L_p$), respectively. In deep water the phase velocity of the spectral peak c_p can be written in terms of the spectral peak frequency as

$$c_p = \frac{g}{2\pi f_p}. \quad (7)$$

Combining this with the relationship between deep-water wavelength and celerity, we have

$$L_p = \frac{2\pi c_p^2}{g}. \quad (8)$$

Or, since u_r is equal to c_p ,

$$z_r = \frac{2\pi\lambda u_r^2}{g}. \quad (9)$$

Solving for u_r , we obtain

$$u_r = \frac{u_{10} \ln\left(\frac{2\pi\lambda u_r^2}{gz_0}\right)}{\ln\left(\frac{10}{z_{010}}\right)}. \quad (10)$$

Once the value for λ is established, this equation has only two unknowns, u_r and z_0 at 10 m. Since the results of [Ewing and Laing \(1987\)](#) suggest that the scaling of spectral energies is consistent somewhere near 16 m s^{-1} , we assume here that u_r will approximately equal u_{10} at this value. This yields a value of 0.065 for λ , which implies that the approximate limit for fully developed waves occurs when the wind speed as a level of 0.065 times the wavelength at the spectral peak is equal to the phase speed of the spectral peak. This is consistent with the tentative assumption made earlier in this section that most of the wind input into the wave field comes from winds relatively close to the surface.

In order to close the above system of equations, it is necessary to specify a relationship between z_0 and u_* . For simplicity, we shall use the Charnock form

$$z_0 = 0.015 \frac{u_*^2}{g} \quad (11)$$

for this purpose. If we were attempting to describe the behavior of wind input over a broad range of wave age (c_p/u_r), it might be necessary to incorporate a wave age dependency in [Eq. \(10\)](#); however, since we are only treating the fully developed limit, this should not be required. This system of equations can be solved iteratively, for any specified value of u_{10} . Since the argument containing z_0 is inside a logarithm function, the sensitivity of the solution for u_r to the exact value of the coefficient in [Eq. \(11\)](#) is fairly small.

An alternative scaling law for fully developed seas is also implicit in third-generation wave models that use a formulation of the type

$$S_{\text{in}} \sim \text{Max}\left(0, \frac{\epsilon u^*}{c} - 1\right), \quad (12)$$

where ϵ is a universal constant, taken as 28 in WAM. Combining the previous argument that u_r equals the phase velocity with [Eq. \(12\)](#) yields a relationship between u_r and u^* for fully developed conditions

$$u_r = c = \epsilon u^* \quad (13)$$

if these scaling forms are equivalent. [Equation \(5\)](#) also provides a relationship between u_r and u^* since

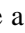
$$u_r = \frac{u^*}{k} \ln(z_r/z_0). \quad (14)$$

When combined with [Eq. \(8\)](#) after a little manipulation, this yields

$$\exp\left(\frac{ku_r}{u^*}\right) = \frac{z_r}{z_0} = \beta \left(\frac{u_r}{u^*}\right)^2, \quad (15)$$

where β is a dimensionless constant. Since the ratio of u_r to u^* enter into the different sides of this equation in different powers, this ratio must be a constant for [Eq. \(14\)](#) to hold. As a simple verification of this, since both u^* and u_r are calculated as part of the iterative solution to [Eq. \(9\)](#), this ratio can be evaluated numerically. The estimated value for ϵ for u_{10} ranging from 1 to 30 m s⁻¹ is within 0.01 of the constant value 24.18, which is within the numerical accuracy of the solution method used. Thus, it appears that the use of either a dynamically scaled wind input level or a friction-velocity scaling for fully developed conditions should produce precisely the same results. It should be noted here that this equivalency has been shown explicitly only for the case of a simple Charnock-type drag law. However, since the effects of wave age on drag tend to be written as a product of a friction-velocity term and a wave age term and since fully developed wave conditions represent a fixed wave age, this equivalency may also hold for this latter class of drag laws.


3. Results and discussion

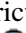
Before proceeding further, it is important to reiterate that discussions and analyses presented in this section are specific to fully developed situations and are not intended for active wave growth, fetch-limited conditions, swell decay, or, in fact, any other situations which differ from the assumptions posed in [section 2](#). [Figure 3](#)  gives the estimated values of u_r as a function of u_{10} based on the solution to the system of equations derived above. A best-fit power-law relationship between u_r and u_{10} , where the units of u_{10} and u_r are meters per second and the units of f_{fd} are hertz, is given by

$$u_r = 0.516u_{10}^{1.244} \quad (16)$$

If we hypothesize that the wind speed at the dynamically scaled height is the proper scaling parameter for the peak frequency of the spectrum in fully developed wave conditions, we can substitute estimates of u_r in place of u_{10} for the v values in Ewing and Laing's data,

$$v' = \frac{u_r f_p}{g} = \frac{u_r}{u_{10}} v.$$

[Figure 4](#)  shows the resulting $v'-u_r$ relationship, along with a linear regression line. The linear correlation coefficient for this relationship is 0.013, which is not even significant at the 0.40 level. Thus, it appears that the substitution of u_r into the scaling relationship significantly reduces the wind-speed dependence of v .

In the previous section, it was shown that the use of friction-velocity scaling, assuming a Charnock-type drag law, will yield essentially identical results to those shown in [Fig. 4](#)  based on a u_r scaling. In fact, in this section we could formulate all discussions in terms of either u_r or u^* . We have chosen to focus on the dynamic-height approach, since it is

easier to see a direct physical mechanism for the cutoff of wind input to waves as the phase speed approaches the wind speed than when the phase speed approaches some multiple of the friction velocity. Since the wind input in the WAM model is formulated to follow a friction-velocity scaling law, the equivalency between u_r and u_* might at first seem somewhat in contradiction to the findings of [Cardone et al. \(1996\)](#). From [Fig. 4](#) we would expect the scaling inherent in the third-generation model to provide a better fit to fully developed growth than found in first- and second-generation models since these latter models are formulated only in terms of u_{10} . This apparent paradox can be resolved by recalling that the third-generation model is not actually formulated in terms of a similarity growth law but rather in terms of a balance among the three dominant source terms in deep water. This suggests that the model physics or numerics inherent in the third-generation model tested by [Cardone et al. \(1996\)](#) is not calibrated to follow the simple scaling law for fully developed conditions developed in this paper.

Comparing the patterns in the u - v relationships in [Figs. 2](#) and [4](#) certainly suggests that u_r (or equivalently u_*) is a better scaling parameter for fully developed spectral peak frequencies than u_{10} . However, spectral peak frequencies often exhibit significant variability in nature due to the randomness inherent in sampling over relatively short time intervals. We are then motivated to seek a relationship between u_r and some more stable spectral parameter in order to provide more support for our argument that u_r is better a scaling parameter for fully developed spectra than u_{10} . Since total wave energy is a reasonably stable spectral parameter and since Ewing and Laing include wave height in the information provided in their Table 1, we shall examine relationships between u_{10} and u_r versus wave height to see which wind speed parameter provides a more consistent scaling law for fully developed spectra. If we substitute u_r for u in [Eq. \(1\)](#), we can obtain an estimate for H_r , the estimated fully developed wave height based on winds at a dynamically scaled reference level. Similarly, if we substitute u_{10} for u in [Eq. \(1\)](#), we can obtain an estimate for H_{10} , the fully developed wave height based on winds at a fixed 10-m reference level. [Figure 5](#) shows a plot of H_r versus H_{10} for identical boundary-layer wind conditions. As can be seen here, wave height differences are relatively small at wind speeds under about 17 m s^{-1} (wave heights of about 7.5 m). Above this speed, the deviations increase slowly at first and then grow dramatically. This finding is in agreement with that of Blake (1991), who showed that fully developed wave heights did not exhibit a velocity-squared dependence on wind speed but were better fit by a velocity-cubed relationship.

If fully developed wave conditions are governed by an equation of the form of [Eq. \(1\)](#) and if u_r is an appropriate similarity scaling parameter for such conditions, $\epsilon_r (=gH_s/u_r^2)$ should be nearer to a constant value in the Ewing and Laing data than $\epsilon_{10} (=gH_s/u_{10}^2)$ in this same dataset. [Figures 6](#) and [7](#) show plots of the ϵ_{10} - u_{10} and ϵ_r - u_r relationships, respectively. The ϵ_{10} - u_{10} relationship appears to be very wind speed dependent with a correlation coefficient of 0.694, significant at the 0.001 level. As seen in [Fig. 7](#), the ϵ_r - u_r relationship has a much reduced wind speed dependence than does the ϵ_{10} - u_{10} relationship, with a correlation coefficient of 0.263. Although this is considerably reduced from 0.694, it is still statistically significant at the 0.10 level. The persistence of some correlation between fully developed wave heights and the new reference wind speed suggests that perhaps some of the parameters affecting the solution for u_r , that is, the assumed functional relationship between u_* and z_0 or the 0.065 value for λ should be modified somewhat; however, since the constant of proportionality in the regression equation between u_r and ϵ_r is only 0.002 08, the impact of the wind speed dependence on the fully developed wave height is less than $\frac{1}{2}$ m for all fully developed conditions up to 17 m, if a constant value of 0.21 is adopted for ϵ_r .

Although the Ewing and Laing dataset provides a high quality dataset for characterizing fully developed seas, it consists of only 28 data points. For this reason it is desirable to examine additional datasets in order to see if the pattern of underpredicting extremes is evident in a broader context. Toward this end, we examined an extensive set of comparisons between hindcast and measured peak wave heights in storms compiled by [Khandekar et al. \(1994\)](#) and supplemented by Cardone as part of ongoing wave model evaluations. These storm peak comparisons are all taken from recent studies that utilized a combination of high quality meteorological data and careful reanalysis of wind fields ([Cardone et al. 1996](#)). The model used in these comparisons was an operational, third-generation spectral model. Both tropical and extratropical storms were represented within the total storm population; hence, a wide range of wave ages might be expected to be represented in these comparisons. However, examination of the individual cases revealed that the larger wave heights in this sample were produced by severe extratropical storms in the North Atlantic, in situations where the sea state could be expected to approach its fully developed limit. In some cases it was the existence of a dynamic fetch that moved with the wave field, and not just the size of the storm, that allowed these waves to approach this limit; but in essentially all situations with very large waves, the wave age was very close to or equal to its fully developed value. [Figure 8](#), from the [Khandekar et al. \(1994\)](#) study, shows a comparison of individual peak measured and hindcast wave heights. A best-fit regression between hindcast and measured wave heights in this dataset was obtained to second order as

$$H_{\text{hindcast}} = -0.369 + 1.123H_{\text{measured}} - 0.020H_{\text{measured}}^2$$

Figure 9 shows a comparison of this relationship to the relationship between the u_{10} -based and u_r -based fully developed wave heights derived in the present study. It appears that the characteristic underprediction of extreme waves in these comparisons is consistent with the expected underprediction due to the use of a u_{10} relationship rather than a u_r relationship in its formulation of fully developed wave heights.

Cardone et al. (1996) provide still another set of data with comparisons of hindcast results to measurements in extreme storms. In fact, this study contains results of peak wave comparisons for all gauges along the east coast of North America for two of the most extreme storms of this century. From the values of wind speeds and wave periods in these storms, it can be argued that the wave ages in these comparisons can be characterized as at or very near being fully developed. Thus, we might again expect that the deviations between predicted and measured wave heights will be consistent with differences between u_{10} - and u_r -scaling for fully developed sea states in these models. In the Cardone et al. study, comparisons between measurements and hindcast data were stratified into two groups, one for all measured wave heights less than or equal to 12 m and one for all wave heights exceeding 12 m. Figure 13 in that study shows a plot of average measured wave heights for each storm stratified into these two wave height categories against the modeled wave heights. Cardone et al.'s Fig. 13 is reproduced as Fig. 10 here with the H_r versus H_{10} derived in the present study plotted in the same coordinates. As can be seen here, the underprediction of extreme wave heights in all generations of spectral wave models, as documented in the Cardone et al. (1996) study, is consistent with the expected difference due to the use of u_{10} scaling in their fully developed formulations.

Since wave models are widely used today in the design of offshore and coastal structures, it is interesting to examine how the results of this paper could be incorporated into existing wave models. In first- and second-generation wave models that use a simple constraint on the peak frequency to limit wave growth, new values for peak frequency as a function of the 10-m wind speed can be established from the solution for u_r . A best-fit curve given by

$$f_{\text{fd}} = 3.33u_{10}^{-1.15} \quad (17)$$

where the wind speed must be specified in meters per second can be used to replace the conventional fully developed limits in such models. In third-generation models, a recalibration of all source terms along the lines of the effort by Komen et al. (1984) would be required to bring the model into better compliance with the scaling law found in this paper.

4. Conclusions

Theoretical arguments suggest that a more appropriate scaling parameter for fully developed seas might be based on winds taken from a height above the sea surface dynamically scaled by wave length rather than on winds from a fixed reference height. This is consistent with the empirical findings of Blake (1991) and the theoretical formulation of Jenkins (1993). In this context, the appropriate similarity form for fully developed spectral densities should be written as either

$$\frac{E(f)g^3}{u_r^5} = \epsilon \left(\frac{u_r f}{g} \right),$$

or equivalently

$$\frac{E(f)g^3}{u_*^5} = \epsilon \left(\frac{u_* f}{g} \right).$$

Over a wide range of wave heights, a reasonable approximation for fully developed wave heights can be written in terms of winds at a dynamically scaled reference height as

$$H_{\text{s-fd}} = 0.21 \frac{u_r^2}{g}.$$

In terms of winds at a 10-m reference level, this yields

$$H_{s\text{-fd}} = 0.056 \frac{u_{10}^{2.488}}{g},$$

which is no longer a quadratic function of wind speed.

Results shown here suggest that the use of winds from a constant reference height can lead to a significant underprediction of extreme fully developed wave heights (about 4 m for a 25 m s^{-1} wind speed) and slight overprediction of small to moderate fully developed waves (heights less than about 5.5 m). This pattern is consistent both with the findings of [Ewing and Laing \(1987\)](#) as well as with recent experience in wave model tests in extreme storms ([Khandekar et al. 1994](#); [Cardone et al. 1996](#)). [Equation \(16\)](#) gives a simple linear regression formula for converting 10-m winds to winds at this wavelength-dependent reference level for fully developed conditions; and [Eq. \(17\)](#) provides a rescaled relationship between the fully developed peak frequency and the 10-m wind speed. These relationships can be used to force first- and second-generation wave models toward agreement with a dynamic-height scaling for fully developed conditions. Since third-generation models use a balance of all three dominant deep water source terms to achieve a fully developed limit to wave growth, it appears that these models may have to be recalibrated along the lines of [Komen et al. \(1984\)](#) to be in better agreement with this scaling.

As pointed out in [section 2](#), all relationships presented in this paper are limited to neutral wind profiles for wind speeds in excess of 10 m s^{-1} . At higher wind speeds ($u_{10} > 20 \text{ m s}^{-1}$ or so) buoyancy effects will probably be fairly small since the relative effect of mechanical mixing to the buoyancy forces will be quite high in most cases. At lower wind speeds, the effect of stability on fully developed seas is likely to be significant but is beyond the scope of this study.

Published data and analyses presented here suggest that wave height tends toward an absolute asymptotic limit as fully developed conditions are approached. A subtle but possibly important point to keep in mind here is that we still have not established the existence of a unique, fully developed limit for the directional spectra of wind-generated waves. From theoretical considerations, it is possible to hypothesize that such a stable form might not exist. As shown by [Komen et al. \(1984\)](#), it is possible to obtain an integrated balance among the three dominant source terms in deep water: wind input, nonlinear transfers due to wave-wave interactions, and wave breaking. However, this does not achieve a detailed balance in which the rate of change of energy densities in each small frequency-direction region of the spectrum is identically zero. Due to differences in the functional forms of the three source terms, such a detailed balance appears to be improbable. It is more likely that the form of the spectrum will continue to evolve, but perhaps on a much slower timescale than during active wave growth as this asymptotic limit is approached and passed.

Consequences of the results presented here could be very significant in terms of the applications of wave models to the estimation of design conditions for offshore and coastal structures, particularly in regions of the world where extratropical storms dominate the extremal wave population. In regions dominated by tropical storms, the effect of rescaling fully developed conditions will probably not influence design wave heights significantly, since the maximum waves inside of these storms tend to be duration or fetch-limited rather than fully developed.

Since longer wave periods in a climatology are generated by storm events, which appear to be underpredicted for winds above about 16 m s^{-1} , it is also likely that long-period swell is underestimated globally by all three generations of wave models presently in operational use. This could have important consequences for a wide range of applications of operational wave models today, such as expected depths of oceanic mixing, swell conditions arriving at sites of operations sensitive to wave period, arrival times of swell at these sites, atmospheric-oceanic coupling, and predicted coastal flooding due to wave setup. Given this level of impact, it is hoped that this paper will motivate more detailed and thorough analyses of fully developed wave conditions in the future.

Acknowledgments

The authors wish to acknowledge the Office, Chief of Engineers, U.S. Army Corps of Engineers, for authorizing publication of this paper that was prepared as part of the military RDT&E program conducted at the USAE Waterways Experiment Station. The authors also wish to express their gratitude to Patricia Oldham and Claudette Doiron for their valuable assistance in the preparation of this manuscript.

REFERENCES

Blake, R. A., 1991: The dependence of wind stress on wave height and wind-speed. *J. Geophys. Res.*, **96** (C11), 20531–20545..

Bretschneider, C. L., 1952: Revised wave forecasting relationships. *Proc. Second Conf. on Coastal Engineering*, ASCE, Council on Wave Research..

Bunting, D. C., 1970: Evaluating forecasts of ocean-wave spectra. *J. Geophys. Res.*, **75**, 4131–4143..

Cardone, V. J., and Coauthors, 1984: In search of the true surface wind field during SWADE IPO-1: Ocean wave modelling perspective. *Global Atmos. Ocean Syst.*..

—, R. E. Jensen, D. T. Resio, V. R. Swail, and A. T. Cox, 1996: Evaluation of contemporary ocean wave models in rare extreme events: The “Halloween storm” of October 1991 and the “storm of the century” of March 1993. *J. Atmos. Oceanic Technol.*, **13**, 198–230..

Chalikov, D. V., 1976: A mathematical model of wind-induced waves. *Dokl. Akad. Nauk SSR*, **229**, 1083–1086..

Donelan, M. A., and W. J. Pierson, 1987: Radar scattering and equilibrium images in wind-generated waves with application to scatterometry. *J. Geophys. Res.*, **92**, 4971–5029..

Ewing, J. A., and A. K. Laing, 1987: Directional spectra of seas near full development. *J. Phys. Oceanogr.*, **17**, 1696–1706.. [Find this article online](#)

Hasselmann, K., 1962: On the non-linear energy transfer in a gravity-wave spectrum, 1, General theory. *J. Fluid. Mech.*, **12**, 481–500..

Janssen, P. A. E. M., 1991: Quasi-linear theory of wind-wave generation applied to wave forecasting. *J. Phys. Oceanogr.*, **21**, 1631–1642.. [Find this article online](#)

Jenkins, A. D., 1993: A simplified quasi-linear model for wave generation and air–sea momentum flux. *J. Phys. Oceanogr.*, **23**, 2001–2018.. [Find this article online](#)

Kahma, K. K., and C. J. Calkoen, 1992: Reconciling discrepancies in the observed growth of wind-generated waves. *J. Phys. Oceanogr.*, **22**, 1389–1404.. [Find this article online](#)

Khandekar, M. L., R. Lalbeharry, and V. Cardone, 1994: The performance of the Canadian Spectral Ocean Wave Model (CSOWM) during the Grand Banks, ERS-1 SAR wave spectra validation experiment. *Atmos.–Ocean*, **32**, 31–60..

Kitaigorodskii, S. A., 1962: Application of the theory of similarity to the analysis of wind-generated wave motion as a stochastic process. *Bull. Acad. Sci. USSR Ser. Geophys.*, **1**, 105–117..

Komen, G. J., S. Hasselmann, and K. Hasselmann, 1984: On the existence of a fully developed wind-sea spectrum. *J. Phys. Oceanogr.*, **14**, 1271–1285.. [Find this article online](#)

Miles, J. W., 1957: On the generation of surface waves by shear flows. *J. Fluid. Mech.*, **3**, 185–204..

Pierson, W. J., 1977: The equilibrium range in the spectrum of wind-generated waves. *J. Fluid. Mech.*, **4**, 426–434..

—, and L. Moskowitz, 1964: A proposed spectral form for fully developed wind seas based on the similarity theory of S. A. Kitaigorodskii. *J. Geophys. Res.*, **69**, 5181–5190..

—, G. Neuman, and R. W. James, 1955: Practical methods for observing and forecasting ocean-waves by means of wave spectra and statistics. H.O. Publ. 603, U.S. Navy Hydrographic Office..

Resio, D. T., 1981: The estimation of wind-wave generation in a discrete spectral model. *J. Phys. Oceanogr.*, **11**, 510–525.. [Find this article online](#)

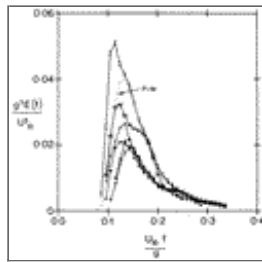
Snyder, R., and C. S. Cox, 1966: A field study of the wind generation of ocean waves. *J. Mar. Res.*, **24**, 141–177..

—, W. Dobson, J. A. Elliot, and R. B. Long, 1981: Array measurements of atmospheric pressure fluctuations above surface gravity waves. *J. Fluid. Mech.*, **102**, 1–59..

Sverdrup, H. U., and W. H. Munk, 1947: Wind, sea, and swell: Theory of relations for forecasting. H.O. Publ. 601, U.S. Navy Hydrographic Office, 44 pp..

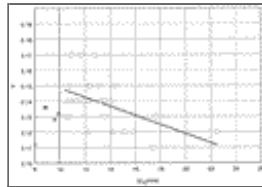
WAMDI Group, 1988: The WAM Model—A third generation ocean wave prediction model. *J. Phys. Oceanogr.*, **18**, 1775–1810.. [Find this article online](#)

Figures



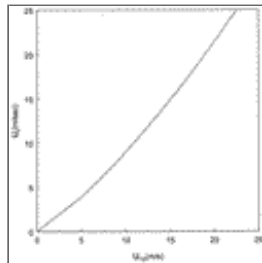
[Click on thumbnail for full-sized image.](#)

Fig. 1. Averaged scaled frequency spectra for six wind speed classes compared to the Pierson–Moskowitz spectrum (from [Ewing and Laing 1987](#)). Key: (+) $u_{10} < 10 \text{ m s}^{-1}$; (*) $10 < u_{10} < 12 \text{ m s}^{-1}$; (Y) $12 < u_{10} < 14 \text{ m s}^{-1}$; (O) $14 < u_{10} < 16 \text{ m s}^{-1}$; (I) $16 < u_{10} < 20 \text{ m s}^{-1}$; (H) $u > 20 \text{ m s}^{-1}$.



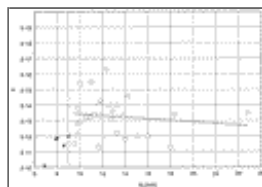
[Click on thumbnail for full-sized image.](#)

Fig. 2. Plot of v against u_{10} from dataset of [Ewing and Laing \(1987\)](#). Closed circles denote cases with wind speed less than 10 m s^{-1} . Open circles denote cases with wind speeds greater or equal to 10 m s^{-1} . The dashed line emphasizes the point of separation between points considered in the regression line and those omitted from consideration.



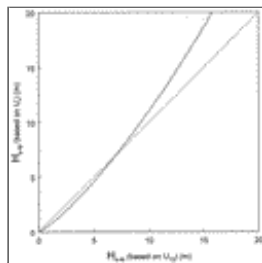
[Click on thumbnail for full-sized image.](#)

Fig. 3. Plot of u_r as a function of u_{10} from [Eq. \(9\)](#).



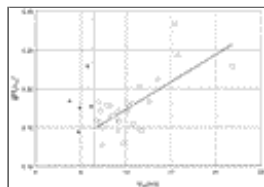
[Click on thumbnail for full-sized image.](#)

Fig. 4. Plot of v' against u_r based on data from [Ewing and Laing \(1987\)](#). Open circles denote cases with wind speeds greater or equal to 10 m s^{-1} . The dashed line emphasizes the point of separation between points considered in the regression line and those omitted from consideration.



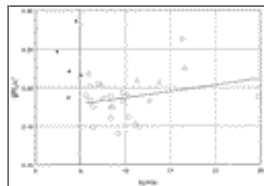
[Click on thumbnail for full-sized image.](#)

Fig. 5. Expected relationship between fully developed wave height based on u_r and fully developed wave height based on u_{10} . The dashed line denotes a 1:1 relationship for reference.



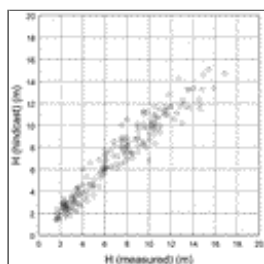
Click on thumbnail for full-sized image.

Fig. 6. Plot of ϵ as a function of u_{10} from the [Ewing and Laing \(1987\)](#) dataset. Open circles denote cases with wind speeds greater or equal to 10 m s^{-1} . The dashed line emphasizes the point of separation between points considered in the regression line and those omitted from consideration.



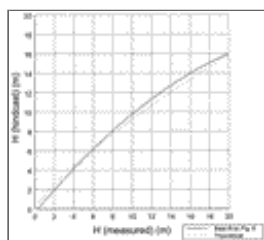
Click on thumbnail for full-sized image.

Fig. 7. Plot of ϵ (estimated from fully developed wave height based on u_r) vs u_r , based on the [Ewing and Laing \(1987\)](#) dataset. Open circles denote cases with wind speeds greater or equal to 10 m s^{-1} . The dashed line emphasizes the point of separation between points considered in the regression line and those omitted from consideration.



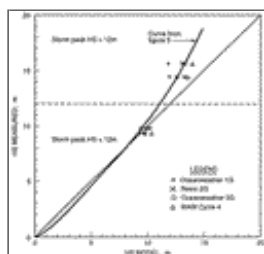
Click on thumbnail for full-sized image.

Fig. 8. Plot of peak measured wave height versus peak hindcast wave height from individual storms compared by [Khandekar et al. \(1994\)](#) and Cardone et al. (1994).



Click on thumbnail for full-sized image.

Fig. 9. Comparison of best-fit quadratic relationship to peak-to-peak comparisons shown in [Fig. 8](#) and the theoretical relationship between fully developed wave heights based on u_r (x-axis coordinate) and fully developed wave heights based on u_{10} (y-axis coordinate).



Click on thumbnail for full-sized image.

Fig. 10. Comparison of theoretical relationship between fully developed wave heights based on u_r (x-axis coordinate) and fully developed wave heights based on u_{10} (y-axis coordinate) to averaged model wave height plots from [Cardone et al. \(1996\)](#).

Corresponding author address: Dr. Donald T. Resio, Coastal and Hydraulics Laboratory, Waterways Experiment Station, Corps of Engineers, Department of the Army, 3909 Halls Ferry Road, Vicksburg, MS 39180-6199.

E-mail: d.resio@cerc.wes.army.mil

[top](#) ▲



© 2008 American Meteorological Society [Privacy Policy and Disclaimer](#)

Headquarters: 45 Beacon Street Boston, MA 02108-3693

DC Office: 1120 G Street, NW, Suite 800 Washington DC, 20005-3826

amsinfo@ametsoc.org Phone: 617-227-2425 Fax: 617-742-8718

[Allen Press, Inc.](#) assists in the online publication of *AMS* journals.